PAPER • OPEN ACCESS

Occurrence, characterization, and transport mechanism of welding fumes particles emitted during the welding process

To cite this article: Norhidayah Abdull *et al* 2024 *J. Phys.: Conf. Ser.* **2688** 012010

View the article online for updates and enhancements.

Occurrence, characterization, and transport mechanism of welding fumes particles emitted during the welding process

Norhidayah Abdull[*1,] Nur Sarah Irina Muhammad[2], , Khairiah Mohd Mokhtar[1], Zarifah Shahri[1]

[1]Faculty of Industrial Sciences and Technology, Universiti Malaysia Pahang AlSultan Abdullah, 26300 Kuantan, Pahang

[2]Honda Malaysia Sdn. Bhd P-3-1, Level 3, Pacific Towers Business Hub, Jalan 13/6, Seksyen 13, 46200 Petaling Jaya, Selangor, Malaysia.

hidayahabdull@ump.edu.my

Abstract. In metalworking processes, welding fumes are a prevalent type of particle aerosols. Particle characteristics, physical factors, and the generation process influence the transport of welding fumes in the air. This research delves into the investigation of welding fumes particles during two types of currents: low current (60A) and high current (130A). The study encompasses the determination of the occurrence and characterization of these particles, as well as estimating their transport mechanisms during the welding process. Direct reading instruments were utilized to measure the mass concentration and the number concentration of welding fumes particles alongside environmental parameters such as relative humidity, air velocity, and air temperature. The size distribution and morphology of the particles were collected through a sampling pump and subsequently analyzed using a Field Emission Scanning Electron Microscope (FESEM). Welding fumes particle transport was predicted by employing variables such as Reynolds number (Re), settling velocity, mechanical velocity, and stopping distance. The welding process's high current (130 A) generates a higher mass concentration (0.122mg/m³) than the low current (60 A) (0.064mg/m³). Notably, for particle size fractions ranging from 0.5µm to 2.0µm, the number of particles generated during high current surpassed that of low current, except for the 0.3µm size fraction. Analysis of the size distribution through FESEM revealed particle sizes of 2.25µm, 2.33µm, and 2.63µm for welding fumes collected during 130A. In contrast, fumes collected during 60A exhibited sizes of 0.45µm, 0.61µm, and 0.60µm. Notably, accumulation of particles were observed, indicating that the fumes collected during 60A consisted of smaller particles classified as fine particles. The particle counts for high and low currents were 283,232,661 count/m³ and 300,604,341 count/m³, respectively. The observed particle shapes appeared agglomerate, comprised of primary spherical particles adhering together through Van Der Waals forces. Reynolds number values (Re=0.0046-0.0223, less than 1) indicated that the motion of fume particles occurred within a laminar flow regime. Furthermore, the movement of particles was influenced by their diameter, with larger particles exhibiting higher settling velocities, smaller mechanical mobility, and shorter travelled distances. In summary, this research sheds light on the intricate transport mechanisms of welding fumes, providing insights into their occurrence, characterization, and transport during the metalworking process.

1. Introduction

Metalworking constitutes a widely employed industrial technique that involves working with elevated temperatures, resulting in the emission of metallic fumes and gases that are potentially unsafe. The global industrial sector annually produces around one million tonnes of weld metal. This process gives rise to an estimated 5,000 tonnes of fumes yearly, calculated from an average fume yield of 0.5% relative to the weld metal produced. Despite the automation and mechanization of the process, an increasing number of welders are being exposed to welding gases due to the development of new welding methods and consumables. The welding process generates fumes and aerosols containing metal particles formed through intricate processes of vaporization, condensation, and oxidation during welding. Airflow can easily affect these particles [1], leading to dispersion beyond the immediate work area. Subsequently, these particles are inhaled by workers, as welding fume particles tend to be highly respirable. The health consequences linked to metal fumes include

conditions such as occupational asthma, bronchitis [2], metal fume fever [3,4], cardiovascular effects [5,6,7], and interstitial pulmonary fibrosis [8], which are contingent on the specific metals present in the fumes.

The production of welding fumes hinges on factors such as voltage, metal, and shielding gas types [9,10]. Emitted fumes pose health risks due to their physical characteristics, and properties like particle size, shape, and density can influence how they are deposited. Ongoing research is dedicated to understanding the implications of welder exposure to typical components of welding fumes. This current study aims to elucidate the movement of welding fumes and the distance travelled by their particles based on their physical attributes. Specifically, the study assesses Gas Tungsten Arc Welding (GTAW) using both low electric current (60A) and high electric current (130A). The outcomes of this study can aid in identifying necessary control measures and fostering a work environment that prioritizes health, safety, and productivity.

2. Methods

2.1 Welding activity

Welding procedures were carried out at a workstation within an educational environment. The Gas Tungsten Arc Welding (GTAW) method was chosen, involving both low electrical current (60A) and high electrical current (130A) settings. GTAW employs a tungsten electrode that remains unconsumed throughout the welding process. A protective inert gas is introduced by initiating an electric arc between this electrode and the workpiece's surface to ensure the integrity of the welding area. In some cases, a filler rod might also be utilized. This technique is especially advantageous for joining non-ferrous materials like aluminium, refractory metals, and exotic alloys. Moreover, it demonstrates remarkable efficiency when used to weld metals with relatively thin cross-sectional profiles.

2.2 Environmental Parameters

IAQ920 Indoor Air Quality Meter (Model 7545, TSI Inc.) with anemometer with hot wire was employed to measure the physical parameters such as relative humidity, air velocity and temperature. The 7545 model simultaneously measures and data logs multiple parameters with response times of 10 seconds. The sampling duration was recorded according to the arcing time. The hot wire was located 50 cm distance from the welding activity. This instrument comes with the special software "LogDat2 Downloading" software which utilizes to transfer the data from instrumentation to the computer.

2.3 Occurrence of Welding Fumes
2.3.1 Mass Concentration of Welding Fumes

The measurement of mass concentration in welding fumes was accomplished using a portable handheld device known as Dustmate (manufactured by Brand Turnkey). The Dustmate utilizes a light scattering technique to gauge the mass concentration of welding fumes and particulate matter within the size spectrum of inhalable, thoracic, and respirable particles. The mechanism of the device involves pulling ambient air samples into its system through a built-in pump. The microprocessor regulates this pump to maintain a consistent flow rate of 10 cubic centimetres per second (equivalent to 600 cubic centimetres per minute). The air laden with welding fumes is directed through a photometer and exposed to a laser beam before passing through a filter that removes the fumes. This purified air is then directed back to the pump.

2.3.2 Determination of Number Concentration of PMs

A Six-Channel Hybrid Handheld Particle Counter (HPC; HPC600, HalTech Inc.) measured the particle number concentration of welding fumes. This handheld laser particle measures welding fumes suspended in the air by pulsing the signals emitted from laser light scattering off aerosol particles, which are processed and counted based on digital signal processing. The results displayed in number concentration (particles/cm3) of the Particle Counter Analyzer, which detected the particle number concentration with the particle sizes of 0.3 mm, 0.5 mm, 0.7 mm, 1 mm, 2 mm, and 5mm. The differential mode was employed to get the number of particles of the exact range of particles in the time interval of 11 seconds.

2.4 Characterization of Welding Fume via Morphological Analysis

A mixed cellulose ester (MCE) filter measuring 37 mm in diameter and featuring a pore size of 0.8 microns was employed to collect welding fumes. Following the OSHA Technical Manual (OTM) 2008, all cassettes must be meticulously sealed by encompassing the inlet and outlet components. This meticulous sealing ensures the samples' integrity and includes comprehensive details to facilitate straightforward identification during the subsequent analysis process. Subsequently, the gathered filters underwent examination through a Field Emission Scanning Electron Microscope (FESEM). This advanced microscopy technique offers detailed insights into the particle size and shape at magnification levels spanning from 10x to 300,000x.

2.5 Transport of Welding Fume

Newton's Resistance Law

Newton formulated an equation to describe the force that opposes the movement of a sphere through a gas medium. The distance traveled by the sphere is proportional to the displacement of the surrounding gas volume caused by the sphere's motion. This derivation is grounded in gas inertia and does not account for molecular viscous friction.

Following information from the National Aeronautics and Space Administration (NASA), the aerodynamic resistance experienced by an object is influenced by multiple factors such as its shape, dimensions, orientation, and flow conditions. All these variables contribute to the overall value of the drag within the drag equation. In the context of a spherical particle following Stokes Law, the drag force expression remains applicable for aerosols within the surrounding atmospheric conditions, as illustrated by Eq. 1:

$$F_D = 3\,\pi\mu d_p V_p \tag{1}$$

In the context of these equations, where FD represents the drag force, dp stands for the particle diameter, VP represents the particle velocity, and μ signifies the dynamic viscosity coefficient of the gas. For conditions where the Reynolds number (Re) is less than 1, such as air at 1013 kPa and 293 K, the dynamic viscosity coefficient (μ) is approximately 1.81×10^{-5} Pa s.

Several assumptions underlie the relationships mentioned above. These include considering a particle as a rigid sphere, the dominance of Stokes Law or a negligible inertial force in comparison to viscous force, the fluid's continuum nature, unobstructed flow without wall effects, low Mach number flow or a constant density of air, and the presence of steady-state flow. Consequently, Newton's assumption that the drag coefficient (CD) remains constant is applicable when dealing with high Reynolds numbers ($Re > 1000$).

Reynolds numbers

$$Re = \rho g V dp \mu \tag{2}$$

Drag Coefficient

$$CD = \frac{24}{Re} = \frac{24\mu}{\rho dp Vp} \tag{3}$$

Considering dp as the sphere's diameter, VP represents particle velocity, and ρg denotes the gas density, with μ being the dynamic viscosity coefficient of the gas.

According to explanations provided by NASA, the drag coefficient serves as a dimensionless value that encompasses the intricate interplay of various factors influencing drag. The drag coefficient and associated drag equation can determine the drag experienced by an object with a similar shape across different flow conditions as long as specific flow similarity parameters align. An essential assumption in the derivation of Stokes' law was the absence of relative gas velocity at the particle's surface. However, this assumption becomes invalid as particle sizes decrease to the point where they approach the mean free path of the gas.

Settling Velocity

Upon release into the air, a particle reaches its terminal settling velocity—a state where it maintains a constant speed and the drag force exerted by the air on the particle, denoted as FD, precisely balances the gravitational force, denoted as FG.

Gravitational Force

$$F_G = mg = \frac{\pi}{6}\rho_p d_p^3 g \qquad (4)$$

Terminal Settling Velocity

$$V_s = \frac{\rho_p d_p^2 g}{18\mu} \qquad (5)$$

Considering variables such as m for mass, g representing the acceleration due to gravity, ρ_p denoting particle density, d_p as particle diameter, and μ indicating the dynamic viscosity coefficient of the gas.

Mechanical Velocity

Regarding mechanical velocity, given that the resistance force by Stokes' law scales with the particle velocity, the particle's mobility can be described as follows. Mobility, represented by the term "B," denotes the relationship between a particle's terminal velocity and the steady-state force responsible for generating that velocity. Hence,

$$B = \frac{V}{F_D} = \frac{1}{3\pi\mu d_p} \qquad (6)$$

Whereas F_D is drag force, d_p is diameter of sphere, V_P is particle velocity, μ is dynamic viscosity coefficient of the gas

Stopping Distance

A particle's term "stopping distance" is the initial distance from the critical surface, where the particle's initial velocity is directed. This distance represents the extent to which the particle experiences deceleration due to various acting forces until it comes to a halt and changes direction. In simpler terms, the stopping distance encompasses the path the particles cover before they cease motion.

$$\tau_p = \frac{\rho_p d_p^2}{18\mu} \qquad (7)$$

Whereas τ_p is particle relaxation time, V_{po} is initial particle velocity and μ dynamic viscosity coefficient of the gas.

3 Results and discussion

3.1 Environmental parameters

Table 1 shows the average air velocity value, temperature and relative humidity detected in the sampling area. From Table 1, the air velocity was 0.20 m/s at the sampling point. The sampling point that recorded the air velocity was located between the side entrance (shutter door) and their working area, surrounded by barriers that prevent maximum airflow from entering the workstations. The air velocity was vital because it may affect the fumes' particle distribution, which welders can inhale [11]. The mean of air velocity measured (0.20 m/s) does not exceed the standard limit stated in the Industry Code of Practice on Indoor Air Quality [ICOP IAQ] (DOSH Malaysia, 2010).

Table 1: Mean of air velocity, temperature, and relative humidity

Environmental parameter	Mean	Acceptable range based on ICOP IAQ 2010
Air velocity [m/s]	0.20	0.15 – 0.50
Temperature [°C]	27.9	23 – 26
Relative humidity [%]	70.9	40 – 70

The recorded temperature at the sampling location was 27.9 °C, surpassing the permissible threshold. It might be attributed to the sampling point's proximity to the entrance, compounded by the wide opening of both doors during that period. Notably, temperature can potentially impact the size of welding fume particles carried through the air [11]. Regarding relative humidity, the recorded average figures for the sampling point hovered around 70.9%. According to [12], relative humidity undergoes considerable fluctuations in response to temperature shifts, even when the water vapour content remains constant. It's worth mentioning that the observed relative humidity went beyond the acceptable range outlined in ICOP IAQ and documented in Table 1. Furthermore, the workstations lacked fans for ventilation enhancement. The ventilation process relied solely

on natural means, such as open windows, to disperse warm air. However, the extent of window opening remained limited.

3.2 Occurrence of welding fumes

Based on the results in Figure 1, all the size fractions ranging from 0.5μm to 2.0μm showed that the number of particles generated during high current was higher than during low current except for the size fraction of 0.3μm, the number of particle counts for high current and low current is 283232661 count/m³ and 300604341 count/m³ respectively. Variability in particle counts and fraction is due to the temperature differences in the welding environment which affect particle formation and dispersion. High-current welding generates more heat, potentially leading to higher temperatures in the vicinity of the weld, which can influence the volatility of certain elements and compounds in the base and filler materials [12]. The current (one of the welding process parameters) also influences the physicochemical characteristics and generation rate of welding fumes, which consequently affects its neurotoxic potential due to the alteration of the fume profile. Literature has demonstrated dopaminergic neurotoxicity attributed to the welding process parameters [13]. However, further investigation needs to be conducted to prove that the greater number of particles produced from high current in this study may cause dopaminergic neurotoxicity.

Figure 2 shows the mean concentration for inhalable, thoracic, and respirable particles are 0.30 mg/m^3 ($\pm$0.1 mg/m^3), 0.21 mg/m^3 ($\pm$0.008 mg/m^3) and 0.009 mg/m^3 ($\pm$0.005 mg/m^3), respectively. The mass concentration of inhalable fume particles is higher than thoracic and respirable particles; however, the concentration reading permitted the permissible exposure limit of 8 hours. The mass concentration of fumes particles during 130A (0.122mg/m³) was higher than during 60A (0.064mg/m³) shown in Table 2. It indicates that welding currents significantly affect the generation rate of particles, the higher the fume generation rate, the more dust is produced [14]. Despite that, the mass concentration results clearly show the fumes particles for both 130A and 60A do not exceed the Occupational Safety and Health Administration Permissible Exposure Limit-8-hour Time Weighted Average (OSHA PEL 8-TWA) of 0.50 mg/m³.
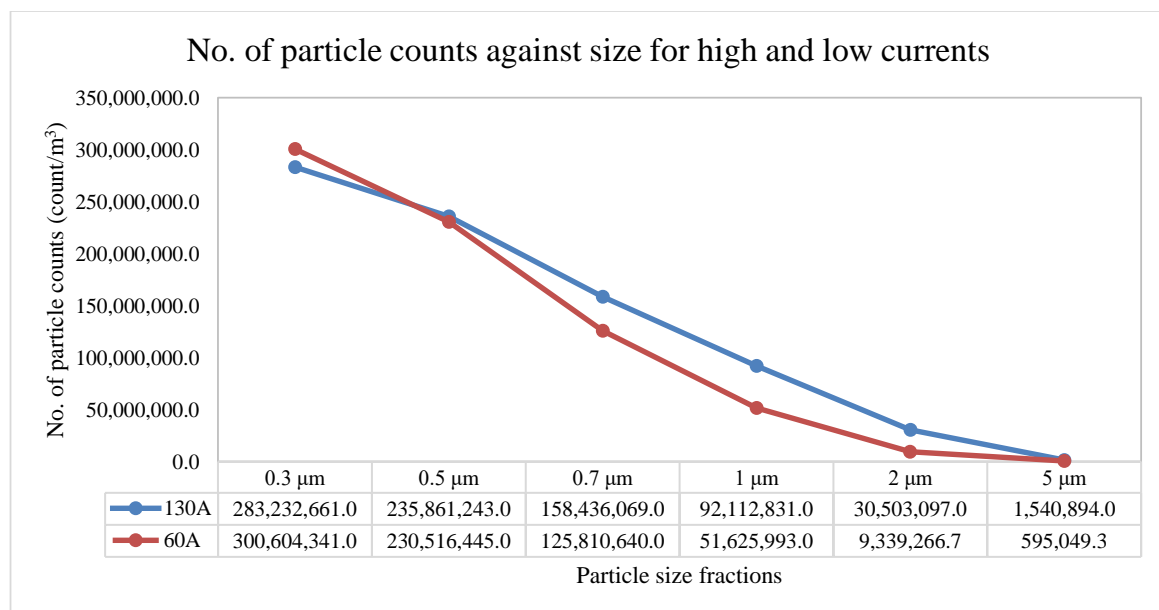

No. of particle counts against size for high and low currents

	0.3 μm	0.5 μm	0.7 μm	1 μm	2 μm	5 μm
130A	283,232,661.0	235,861,243.0	158,436,069.0	92,112,831.0	30,503,097.0	1,540,894.0
60A	300,604,341.0	230,516,445.0	125,810,640.0	51,625,993.0	9,339,266.7	595,049.3

Figure 1: Number of particle counts (count/m^3) based on the size fractions (μm)

Table 2: Mass concentration (mg/m^3) of respirable dust for 130A and 60A

Sampling points	Mass Concentration [mg/m³]		
	130A	**60A**	**OSHA PEL-TWA**
1	0.140	0.064	
2	0.110	0.062	0.50
3	0.116	0.065	

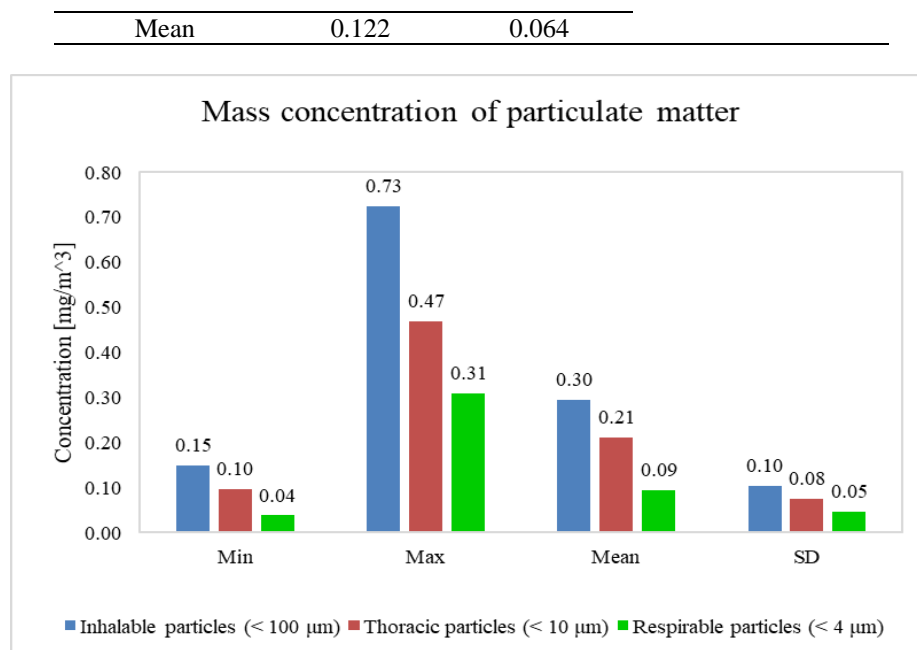|	Mean	0.122	0.064

Figure 2: Mass concentration of inhalable, thoracic, and respirable size particulate matter.

3.3 Morphology of welding fumes

The morphology assessment of welding fumes gathered from various current settings (A) was examined by FESEM. Figures 3 and 4 exhibit the chosen, representative depictions of the detected particles. The acquired FESEM images confirmed the prevalence of primary particle clusters in welding fumes derived from the gas metal arc welding (GMAW) procedure, regardless of whether high or low voltage was employed. It is noted in [15] that welding fume particles stem from processes like evaporation and micro spatter, resulting in a non-uniform composition structure.

Determining the effective particle diameter of an aggregate involved calculations based on the two-dimensional image's area [16]. Notably, the measurements for particles collected at 130A showed larger dimensions, specifically 2.25μm, 2.33μm, and 2.63μm. Conversely, particles collected at 60A exhibited smaller sizes, measured at 0.45μm, 0.61μm, and 0.60μm. However, particle clusters indicate that fumes obtained during 60A feature smaller particle sizes, which fall within the category of fine particles. Figure 3 showcases numerous spherical shapes within the agglomerates, while Figure 4 illustrates that aerosols generated during 130A tend to be arranged as inhomogeneous, chain-like agglomerates of primary particles. Particle size and morphology are important determinants of the hazard potential of the welding fumes to the welder's health, as they provide insight into how deep the particles may penetrate the lungs [17]. As mentioned in [18], fine particles smaller than 2.5 μm can easily enter the respiratory system and lodge in the alveolar region of the lungs, resulting in respiratory disorders.

Particles resulting from nucleation processes are termed primary particles in agglomerates or aggregates exhibiting fractal structures. Aggregates refer to collections of coalesced primary particles, while agglomerates are formed when primary particles unite due to electrostatic or van der Waals forces. A separate study [16] demonstrated that smaller welding fume particles often come together in the air before being collected, forming larger particle agglomerates that simulate the behaviour and impact of larger spherical particles. These agglomerates appear reminiscent of foam or finely entangled hair when observed through micrographs. Agglomerates represent a conglomeration of primary particles or aggregates where the combined surface area does not markedly deviate from the sum of specific surface areas of individual primary particles. Although agglomerates lack fixed dimensions, their size and configuration are modifiable. As [19] suggests, external factors like temperature, pressure, pH levels, and viscosity may induce variations in agglomerates. Notably, the density of agglomerates is contingent upon the particle size distribution of the primary particles.
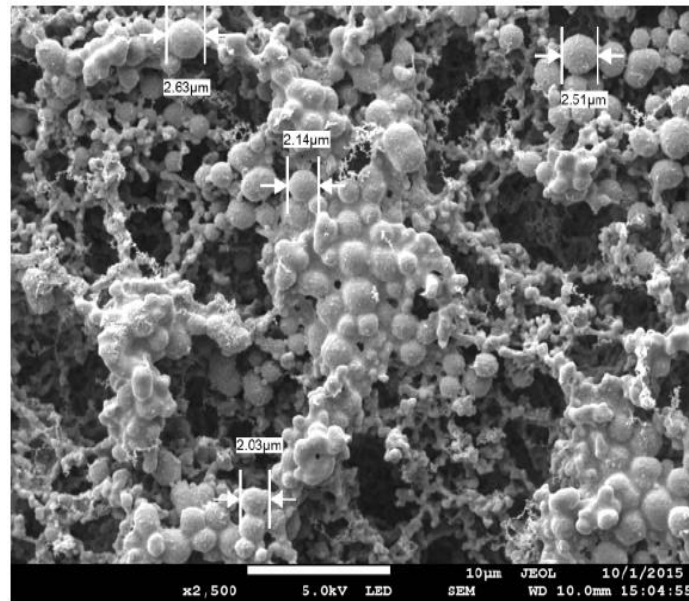
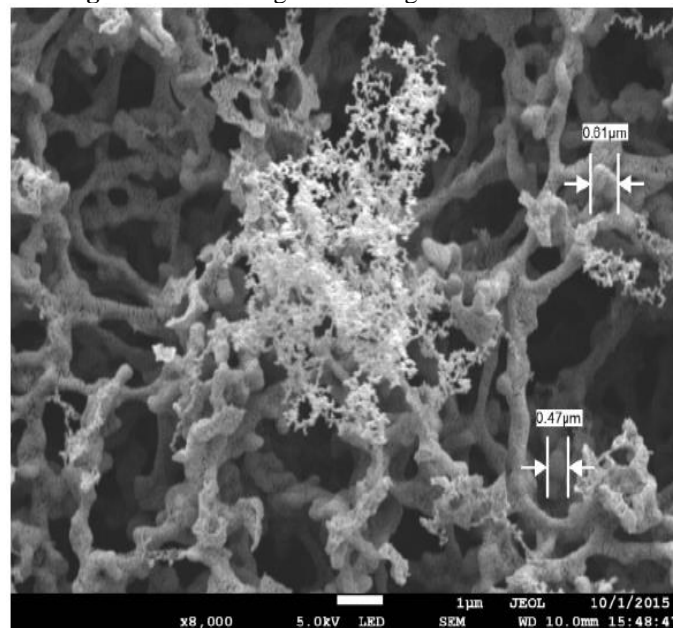**Figure 3:** SEM image of fumes generated from 130A

Figure 4: SEM image of fumes generated from 60A

However, further insight into fume formation mechanisms in arc welding remains necessary. It's posited that particle charging's impact is negligible in the case of a pure argon shielding gas, as electron density remains minimal during particle coagulation at low temperatures [20]. Nonetheless, the presence of metal vapour in low concentrations significantly enhances electron density at lower temperatures due to the low ionization potential of metal atoms. Numerous agglomerates are evident in the samples depicted in Figure 3. Nevertheless, they exhibit slight dissimilarity from the agglomerates featured in Figure 2. These agglomerates are generally densely packed and, in certain instances, form substantial, consolidated round conglomerates comprised of multiple fume particles of varying sizes.

In the context of the GMAW process, fume formation is predominantly driven by electrode evaporation, aligning with the electrode tip's elevated temperature compared to the weld pool. Despite potentially higher bulk temperatures, smaller droplets generated during spray or pulsed transfer possess cooler surface

temperatures than larger droplets, as seen in globular transfer. This phenomenon arises due to a lesser barrier to heat transfer from the arc spot to the liquid-solid interface of the electrode [16].

3.4 Transport of particulate matter

Welding fumes particles are fine particles with a diameter of up to 10μm. Due to their small size cannot be seen with the naked eye, but they are present in the air. Therefore, it is essential to characterize the motions of fumes in the air which deduced from the air velocity, relative humidity, temperature, particle size and density. Those motions include the type of particle motion, the suitable Law to be applied, drag force, settling velocity, terminal settling velocity, mechanical velocity and the stopping distance of the fumes particles in the air. The flow of particle motion may be laminar or turbulent flow. Reynolds number is an appropriate dimensionless quantity for the distinction between laminar or turbulent. It is the ratio of the inertia to viscous effects in the flow. The transition from laminar to turbulent flow may occur at various Reynolds numbers, depending on how much flow is disturbed. If the Reynolds number is very small ($Re \leq 1$), it is an indication that the viscous forces are dominant in the problem, and the inertial effects may be neglected [21].

Newton's resistance equation is valid in the turbulent flow regime ($Re > 1000$), where inertial forces are much larger than viscous forces. The drag coefficient, CD, has a nearly constant value of 0.44. However, Newton's Law is invalid when small particle size and low velocity are involved, the Reynolds number is small, and the flow is laminar. Under this condition, inertial forces are negligible compared to viscous forces. Therefore, Stokes' Law shall be used. Based on the results in Table 3, the Reynolds number (Re) obtained for 130A and 60A are 0.0223 and 0.0046, respectively. The value Re obtained for both currents is less than 1 ($Re \leq 1$) showing the motion flow of the fume particles is a laminar flow. This laminar flow regime implies less mixing and dispersion of fume particles, which may promote speedier settling and predictable deposition patterns [22].

Table 3: The Reynolds Number (Re) versus Drag Coefficient (C_D) Value

Current	Re	C_D
130A	0.0223	1.076×10^3
60A	0.0046	5.217×10^3

When the force acting on the fume's particle was determined by using the Reynolds number, the movement of the fume particle could also be determined. When fumes particle is released into the air, it will settle due to gravity and thus, the velocity increases [23]. As the particle's speed increases, the drag force acting on it increases, resulting from the substance it passes through. At some speed, the drag force will equal the gravitational pull on the object. At this point, the particle ceases to accelerate and continues falling at a constant speed called settling velocity. Particles that move downward with greater than settling velocity will slow down until they reach settling velocity. The drag exerted on it depends on the projected area; particles with a larger projected area relative to mass have a lower settling velocity than particles with a smaller projected area relative to mass [23].

The calculated value for Drag Force, Settling Velocity, Terminal Settling Velocity and Mechanical Velocity of fume particles, 130A and 60A, was tabulated in Table 4. Settling is the process of particulates settling to the bottom and forming sediment. Particles that experience gravitational force or centrifugal motion will tend to move uniformly in the direction exerted by the force. However, the applied force is usually unaffected by the particle's velocity, whereas the drag force is a function of the particle velocity. Based on the result in Table 4, the Drag Force of fumes particle for 130A is higher, which is 5.732×10^{-11}N when compared with during low voltage which is 1.173×10^{-11}N.

Table 4: The value of Drug Force (FD), Settling Velocity (SV), Terminal Settling Velocity (VTS), and Mechanical Velocity (MV) of fume particle.

Current	Drag Force, FD [N]	Settling Velocity, FG [g.m/s^2]	Terminal Settling Velocity, TSV [m/s]	Mechanical Velocity, MV [mN^{-1}s^{-1}]
130A	5.732×10^{-11}	7.101×10^{-7}	1.855×10^{-7}	2.613×10^9
60A	1.173×10^{-11}	8.546×10^{-9}	1.187×10^{-8}	1.389×10^{10}

Other than that, for the gravitational force (FG) and Terminal Settling Velocity (TSV), the velocity of fumes particles during high current is higher when compared with low current as the values of FG and TSV during 130A are 7.101×10^{-17} g.m/s^2 and 1.855×10^{-7} m/s. In contrast, the values of FG and TSV during 60A are 8.546×10^{-19} g.m/s^2 and 1.187×10^{-8} m/s. Their diameter influenced the movement of particles. The settling velocity will increase along with the diameter of the fume's particles. The larger the diameter of particles, the higher the value of settling velocity.

Furthermore, mechanical velocity is calculated to know the movement of particles to have a constant motion in the air, either more quickly or not. The smaller the fumes particles, the larger the mechanical mobility and easier for the particles to move. Based on Table 4, the mechanical velocity was higher during high voltage, 2.613×109 m$N^{-1}s^{-1}$ and lower during low voltage, 1.389×10^{10} m$N^{-1}s^{-1}$. Thus, it clearly shows that the fume particles move easily during 60A compared to during 130A.

Stopping distance determines the maximum distance of a particle with an initial velocity that will travel in the still air without any external forces, where only drag force is acting on the particle. The calculated value of stopping distance for both 130A and 60A was tabulated in Table 5. It shows that the stopping distance during high current is 1.513×10^{-9} m, whereas the stopping distance during low current is 9.683×10^{-11} m. Based on Table 5, when compared with the diameter of fumes particles, particles formed during 130A had a larger diameter, which was 2.40×10^{-6} m therefore, the distance travel was shorter when compared with the particles during 60A as the diameter was smaller, which was 0.55×10^{-6} m.

Table 5: Stopping distance (S) of particles based on the diameter of particles.

Current	Diameter of fume, Dp [m]	Stopping Distance, S [m]
130A	2.40×10^{-6}	1.513×10^{-9}
60A	0.55×10^{-6}	9.683×10^{-11}

However, the air velocity may have affected the stopping distance of the fume's particles. Fume particles can be extensively dispersed by high air velocity, delaying their quick settling, while high relative humidity can make fume particles hygroscopic and accelerate settling. High humidity can also encourage condensation and particle agglomeration, which can result in heavier, bigger particles that settle more easily, especially at lower air speeds [24]. The interplay between air velocity and relative humidity is a critical factor in the dispersion, settling, and interaction of fume particles in many environmental and industrial contexts.

During the welding process, the effective way to reduce welding fumes exposure is by implementing engineering control. The welders' workstations should be well-ventilated in the first place. The workstations can be ventilated through prevailing winds. Air movement can provide natural ventilation. Its effectiveness depends on the weather. In indoor locations and confined spaces, draft fans or air movers provide general or dilution ventilation. Local exhaust ventilation (LEV) is one of the most effective ventilation systems. It is suitable for all situations that generate heavy metal fumes and for stainless steel or plasma-arc welding. Vent hoods can provide local exhaust ventilation. The effectiveness of LEV depends on the distance of the hood from the source of gases and fumes, on the air velocity and the hood placement. Before installing any ventilation, it is crucial to understand the types of contaminants produced, work procedures and characteristics of the work area to have a proper design and location of the ventilation systems. The airflow must be checked regularly with measuring instruments to ensure the systems work correctly. The exhaust discharges outside the room or confined space when using vent hoods.

Safety training is essential for the welders as a personal protection. Knowledge of ventilation system inspection related to fan operation and filter cleaning before work begins is vital. Welders must also be familiar with welding electrodes' Safety Data Sheet (SDS) to know the inherent hazards. Using respiratory protective equipment (RPE) is important as the fume is hazardous. Furthermore, it is the responsibility of the management to provide the RPE for them. All respirators may be uncomfortable for first-time users. Thus, selecting RPE is essential so that wearing it will be more bearable. Ensuring that the respirator is adequately fit is crucial to prevent hazardous materials from leaking into the breathing air. To protect the welders from hazards, a shielding mask should be supplied to protect them from ultraviolet radiation flashes, "weld-spatter", or grinding. Gloves are also one of the necessary PPE to prevent burns from sparks and electric shocks, and for foot protection, it is required to wear proper safety shoes when near and at the workstations.

4   Conclusion

Welding process is one of the most hazardous processes in manufacturing industry due to the fumes generate during the process. It is important to study the physical properties of welding fumes and the morphology of particles for low voltage and high voltage welding activity. Theoretically, when the voltage increases, the number of particles also increases and more generation of smaller size particles. Overall trend of the graph showed that the number of particles is inversely proportional to the size fraction of particle. The highest count of particles is in between the size fraction of 0.3 μm and 0.7 μm. As for the mass concentration of fume particles, the higher voltage showed higher mass concentration. The shape of particles formed during high voltage was in agglomerates form and the size of fume particles was bigger than the fume particles formed during low voltage which was 2.44 μm. Fume particles formed during low voltage was observed to be in chain-like agglomerates which can be said as accumulation of cluster of primary particles. The particle size during low voltage also appeared to be smaller which was 0.55 μm. It was said that the density of agglomerates depends on the particle size distribution of the primary particles.

The flow motion of the fume particles was laminar flow which determined by the small Reynolds number (Re $\leq$ 1). Besides, due to the small Re, the drag coefficient indicates that Newton's law can be neglected and the Stokes' law shall be used. For velocity of fume particles, as the speed of the particle increases, the drag force acting on it, resultant of the substance it is passing through also increases. The values of Drag Force, Gravitational Force and Terminal Settling Velocity were higher when compared to low voltage. The settling velocity will increase along with the diameter of the particles. Other than that, for mechanical velocity, a smaller particle has larger mechanical mobility. Therefore, mechanical velocity for particles during low voltage was larger compared to high voltage as the particles size for low voltage was smaller. It clearly showed that fume particles move easier during low voltage. As for stopping distance of fume particles, larger diameter of particles has higher settling velocity and shorter distance travelled. It illustrated that fume particles during high voltage had shorter distance travelled as their diameter was larger compared to fume particles formed during low voltage.

Acknowledgement

References

[1]   Olivera Popović a,n, Radica Prokić-Cvetković a, Meri Burzić b, Uroš Lukić b, Biljana Beljić, Fume and gas emission during arc welding: Hazards and recommendation, Renewable and Sustainable Energy Reviews. 37 (2014) 509 – 516.

[2]   Lillienberg, L., Zock, J.P., et al., 2008. A population-based study on welding exposures at work and respiratory symptoms. Ann. Occup. Hyg. 52, 107–115.

[3]   Antonini, J.M., Lewis, A.B., et al., 2003. Pulmonary effects of welding fumes: review of worker and experimental animal studies. Am. J. Ind. Med. 43, 350–360.

[4]   El-Zein, M., Malo, J.L., et al., 2003. Prevalence and association of welding related systemic and respiratory symptoms in welders. Occup. Environ. Med. 60, 655–661.

[5]   Cavallari, J.M., Eisen, E.A., et al., 2008. PM2.5 metal exposures and nocturnal heart rate variability: a panel study of boilermaker construction workers. Environ. Health 7, 36.

[6]   Fang, S.C., Cassidy, A., et al., 2010b. A systematic review of occupational exposure to particulate matter and cardiovascular disease. Int. J. Environ. Res. Public Health 7, 1773–1806.

[7]   Scharrer, E., Hessel, H., et al., 2007. Heart rate variability, hemostatic and acute inflammatory blood parameters in healthy adults after short-term exposure to welding fume. Int. Arch. Occup. Environ. Health 80, 265–272.

[8]   Yu, I.J., Song, K.S., et al., 2001. Lung fibrosis in Sprague-Dawley rats, induced by exposure to manual metal arc-stainless steel welding fumes. Toxicol. Sci. 63, 99–106.

[9]   Yoon CS, Paik NW, Kim JH. Fume generation and content of total chromium and hexavalent chromium in flux cored arc welding. Ann Occup Hyg. 47 (2003) 671–80.

[10]   Pires I, Quintino L, Miranda RM, Gomes JFP. Fume emissions during gas metal arc welding. Toxicol Environ Chem 88 (2006) 385–94.

[11]   Zhuang J., Liu J., Chen G., Han K., Jiang J., Tian D., Diao Y., Shen H. A numerical study for predicting the maximum horizontal distance of particles' dispersion during transient welding processes. Journal of Building Engineering 71 (2023).

[12]   Djongyang N., Tchinda R., Njomo D. Thermal comfort: a review paper. Renew Sustain Energy Rev. 14(9), (2010) 26-40.

[13]   Sriram, K., Lin, G.X., Jefferson, A.M., Stone, S., Afshari, A., Keane, M.J., McKinney, W., Jackson, M., Chen, B.T., Schwegler-Berry, D. and Cumpston, A., 2015. Modifying welding process parameters can reduce the neurotoxic potential of manganese-containing welding fumes. Toxicology, 328, pp.168-178.

[14]   Takahashi, J., Nakashima, H., & Fujii, N. (2020). Fume particle size distribution and fume generation rate during arc welding of cast iron. Industrial health, 58(4), 325–334.

[15]   Rubino F., Tucci F., Caruso S., Umbrello D., Carlone P. An integrated numerical approach to simulate the filter deposition of the shape distortions in gas metal arc welding. CIRP Journal of Manufacturing Science and Technology 45 (2023) 26-34

[16]   Jenkins N.T., Pierce W.M-G., Eagar T.W. Chemical analysis of particle size distribution. Welding Journal. (2005) 87-93.

[17]   Vishnyakov, V. I., Kiro, S. A., Oprya, M. V., & Ennan, A. A. (2017). Effects of shielding gas temperature and flow rate on the welding fume particle size distribution. Journal of Aerosol Science, 114, 55-61.

[18]   Xing, Y. F., Xu, Y. H., Shi, M. H., & Lian, Y. X. (2016). The impact of PM2. 5 on the human respiratory system. Journal of thoracic disease, 8(1), E69.

[19]   Kato N., Yamada M., Ojima J., Takaya M. Analytical method using SEM-EDS for metal elements present in particulate matter generated from stainless steel flux-cored arc welding process. Journal if Hazardous Materials 424 (2022) 127412.

[20]   Yamaguchi M., Komata R., Furumoto T., Abe S., Hosokawa A. Influence of metal transfer behaviour under Ar and CO2 shielding gases on geometry and surface roughness of single and multilayer structures in GMAW-based wire arc additive manufacturing of mild steel. The International Journal of Advanced Manufacturng Technology 119 (2022) 911-926.

[21]   Munson B.R., Young D.F., Okiishi T.H. Fundamentals of Fluid Mechanics, Fifth Edition. United State: John Wiley & Sons (Asia) Pte Ltd. (2006).

[22]   Oprya, M. & Kiro, S. & Worobiec, A. & Horemans, Benjamin & Larysa, Darchuk & Novakovic, Velibor & Ennan, A. & Van Grieken, R.. (2011). Size distribution and chemical properties of welding fumes of inhalable particles. Journal of Aerosol Science - J AEROSOL SCI. 45.

[23]   Estokava A. & Stevulova N. Chapter 18-Investigation of Suspended and Settled Particulate Matter in Indoor Air. (2012).

[24]   Wang, L.-Y., Yu, L. E., & Chung, T.-S. (2019). Effects of relative humidity, particle hygroscopicity, and filter hydrophilicity on filtration performance of hollow fiber air filters. Journal of Membrane Science, 117561.